Enhanced Primary Droop Controller for Meshed DC Micro-Grids with Overvoltage Protection

A.-C. Braitor, G. C. Konstantopoulos and V. Kadirkamanathan

Abstract— Droop control represents the key grid-forming control strategy in modern micro-grids consisting of multiple distributed energy resources (DERs), implemented at the primary control layer of the hierarchical control architecture. In this paper, an enhanced droop control methodology for meshed DC micro-grids with constant power loads (CPLs) is proposed, which inherits the conventional droop control features and additionally guarantees a crucial overvoltage protection property of each DER unit, independently from each other or the loads. Since one of the main challenges in DC micro-grids is that CPLs introduce negative impedance characteristics that can lead to system instability, in this paper, based on the proposed novel control structure and using nonlinear ultimate boundedness theory, an upper limit for the output voltage is rigorously guaranteed. In addition, asymptotic stability to the desired equilibrium for the closed-loop system is analytically proven, and detailed conditions are derived to guide the control design. Simulation testing is performed for a meshed DC micro-grid to verify the theoretical contribution and the effectiveness of the proposed primary droop controller.

I. Introduction

Nowadays, conventional electrical power grids are witnessing a steady increase of renewable energy sources (RES). Simultaneously, conventional power plants based on synchronous generators, which provide important grid functions such as inherent frequency support from their mechanical inertia or grid restoration capability, are being replaced by RES and energy storage systems (ESS). As a result, these DER units are expected to behave in a similar manner and provide ancillary services to the main grid. Since the majority of the DER units is integrated to the grid via power electronic converters, their desired operation lies on the suitable control design of their converter components.

As DER units are distributed in the power grid, neighbouring DERs and local loads can form small-scale power networks to utilise clean electricity within their premises, resulting in the so called *micro-grids*. Among the different micro-grid types, DC micro-grids are becoming increasingly interesting since most of the DER units operate in DC power, i.e., PV systems, batteries, fuel cells, etc. Hence, the control of the DER converter units within a DC micro-grid is crucial for providing a stable and reliable DC network

architecture, and is mainly formed in a hierarchical control structure [1], [2]. As reported in [3]–[5], the standard primary control approach, that is located at the lower level of the hierarchical control architecture and is responsible for the stability of the micro-grid, is based on the concept of droop control. However, droop control strategies increase the output resistance of the DER units which places them further away from an ideal (current/voltage) source. This results in the local DC bus voltage being more dependent on the load coupled to the system [6].

Particularly, in DC micro-grids, ensuring system stability is a major challenge especially in the presence of CPLs. Unlike passive loads, CPLs, also known as active loads, enable the power conditioning at the load side and behave as negative impedances in the small-signal model analysis; thus, introducing instabilities in a DC micro-grid system [7], [8]. Safe operating regions have been calculated in [6] to provide a useful micro-grid design guideline. Several methods aimed to increase the system stability margin using different approaches, i.e. via introducing passive damping [9], additional filter or energy storage devices [10] to deal with the voltage oscillations at the DC bus, virtual resistance [11] to adjust the current flowing through the source and DC link; virtual capacitance [12] to reduce the size and weight of DC-link capacitor. In all of these approaches in order to guarantee small-signal stability with a CPL, the condition imposed by the impedance inequality criterion must be always met.

Since DC capacitors are customary used at the output of each DER converter unit to stabilize the output voltage, they also introduce a maximum voltage limit. Hence, apart from the theoretical analysis, the need of protecting the power units from overvoltages through control has emerged [13], [14]. In plain words, overvoltages happen when the voltage in a circuit, or part of the circuit, increases above its designed limit, causing potential damage in the converter components or the grid. Potential limitations and the main challenges when experiencing such situations have been discussed in [15]. In [16], a comparison, by means of optimal power flow (OPF), between centralized and local voltage control solutions have been conducted to mitigate the voltage rise impact. Several methods, for instance [17], [18], aim to reduce the active power injected by a source until its local voltage complies with the operational requirements, commonly referred to as active power curtailment (APC). In [19], the authors propose a methodology to identify and locate transient overvoltages using wavelet packet decomposition (WPD) and general regression neural networks (GRNN)

theory. In the same framework, a protection structure for locating any type of fault in meshed micro-grids has been proposed in [20]. However, incorporating the overvoltage protection at the primary control layer, in order to maintain the local DER voltage limitation even during transients, continues to remain an open problem.

In this paper, an enhanced primary droop controller is proposed for meshed DC micro-grids with local CPLs that guarantees an upper limitation for every DER unit local output voltage independently. In particular, motivated by the recently developed state-limiting PI (sl-PI) control in [21], a novel droop control structure is first proposed and analyzed. Using nonlinear ultimate boundedness theory, it is rigorously proven that every node voltage within the DC micro-grid network architecture remains bounded below a desired maximum value. Then, closed-loop stability is analytically investigated and sufficient conditions are derived to inform the control design and ensure a stable DC micro-grid system despite the multiple CPLs. Finally, the theoretical contribution of the paper and the effectiveness of the novel primary droop controller is verified by simulating a meshed DC micro-grid with multiple DER units and CPLs.

The rest of this section introduces some notations and revisits basic graph theory preliminaries used throughout the entire manuscript. Section II introduces the meshed DC micro-grid model with local CPLs. In Section III, the novel droop control strategy is proposed. Closed-loop stability of the entire micro-grid is guaranteed in Section IV, while in Section V the simulation results of a DC micro-grid are presented. Finally, conclusions are drawn in Section VI.

A. Common notations

Let $v \in \mathbb{R}^n$ represent the associated vector of an n-dimensional sequence $(v_1, v_2, \ldots, v_n)$, and $[v] \in \mathbb{R}^{n \times n}$ the associated matrix, whose diagonal entries are the elements of v. Consider $\mathbf{1}_n \in \mathbb{R}^n$ the n-dimensional vector with all entries equal to one, and $\mathbf{0}_{n \times n} \in \mathbb{R}^{n \times n}$ the n-dimensional matrix with all the entries equal to zero. Let $\mathcal{I}$ be the ordered index set, and I_n the identity matrix. For $v \in \mathbb{R}^n$, define the column vector-valued, and diagonal matrix-valued functions $\mathbf{sin}v$, $\mathbf{cos}v$, and $[\mathbf{sin}v]$, $[\mathbf{cos}v]$, respectively.

B. Graph theory preliminaries

Let $\mathcal{G}(\mathcal{V}, \mathcal{E})$ be a weighted undirected and connected loopy graph with the set of vertices $\mathcal{V}$ and the set of edges $\mathcal{E} \subseteq \mathcal{V} \times \mathcal{V}$. The notation $\varepsilon_{ij} = (i, j) \in \mathcal{E}$ denotes the edge that connects the nodes i and j, where (i, j) is an unordered node pair. Since the graph $\mathcal{G}$ is connected, there exists a spanning tree connecting all the nodes of $\mathcal{G}$ (with $n - 1$ edges). The Laplacian matrix of the loopy graph $\mathcal{G}$ is defined as $L_G = L + D$, where D is diagonal and contains the self-loops of each node on the main diagonal.

II. DC MICRO-GRID MODEL

A common meshed DC micro-grid architecture is depicted in Figure 1, consisting of a finite number of nodes n, each of the nodes representing a controllable DER unit supplying a local CPL and connected with each other through resistive
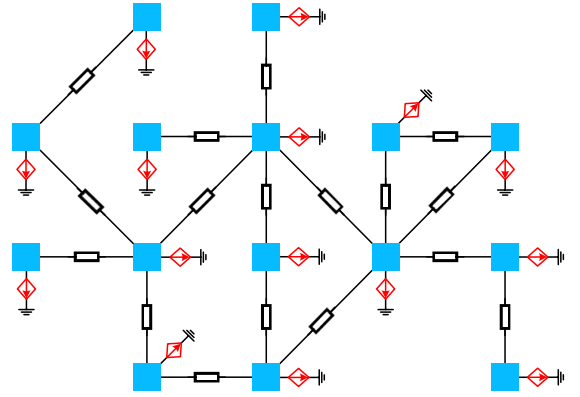

Fig. 1: Generic framework of a meshed DC micro-grid.

lines. Note that if a different micro-grid architecture was considered, where some nodes include a load but not a DER source, the system can still be transformed into the one in Figure 1 using the Kron-reduced network approach [22]. In Figure 2, the model of the voltage source converter that integrates each DER unit with each node j is depicted. The dynamic equations of the capacitor voltages for an arbitrary node j can be obtained by employing Kirchhoff's laws

$$C_j \dot{V}_j = i_{inj} - i_j, \tag{1}$$

where C_j is the output capacitor, V_j is the output voltage, while i_{inj} and i_j represent the input and output current, respectively, with i_{inj} also used as the control input, for $\forall j \in \mathcal{I}$. This is a typical system representation where an inner current controller is applied to the converter, resulting in a fast regulation of the inductor current to the value i_{inj} [2]. One can express the output current of the converter as

$$i_j = \frac{P_j}{V_j} + \sum_{k \in \mathcal{N}_j} i_{jk}, \tag{2}$$

where $\mathcal{N}_j$ represents the neighbourhood of the node j, in the induced graph $\mathcal{G}$ described by the meshed DC network, i.e., $\mathcal{N}_j \in \mathcal{V} : \varepsilon_{jk} \in \mathcal{E}$.

Remark 1. Note that the configuration represents just a generic model of n-sourced units that could be incorporated within the microgrid via different power converter configurations (buck, boost, buck-boost, AC/DC), where a fast inner current control loop is considered.

Considering a steady-state voltage value for the j-th node denoted by V_{je}, by taking the partial derivative of the output current i_j from (2) with respect to the output voltage V_j, one can obtain the symmetric admittance matrix Y of the DC micro-grid, in the following form:

$$Y = \begin{bmatrix} -\frac{P_1}{V_{1e}^2} + \sum_{k \in \mathcal{N}_j} \frac{1}{R_{1k}} & -\frac{1}{R_{12}} & \cdots & -\frac{1}{R_{1n}} \\ -\frac{1}{R_{12}} & -\frac{P_2}{V_{2e}^2} + \sum_{k \in \mathcal{N}_j} \frac{1}{R_{2k}} & \cdots & -\frac{1}{R_{2n}} \\ \vdots & \vdots & \ddots & \vdots \\ -\frac{1}{R_{1n}} & -\frac{1}{R_{2n}} & \cdots -\frac{P_n}{V_{ne}^2} + \sum_{k \in \mathcal{N}_j} \frac{1}{R_{nk}} \end{bmatrix}.$$

If there is no connection between the vertices j and k, i.e., $\varepsilon_{jk} \notin \mathcal{E}$, the corresponding Y matrix entry will be zero, i.e.,
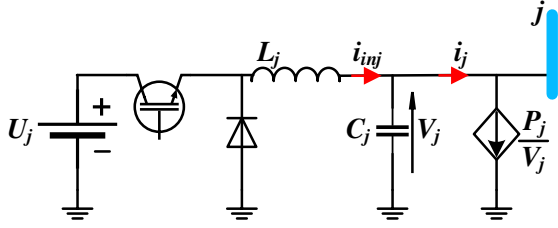
a) Voltage source converter model.
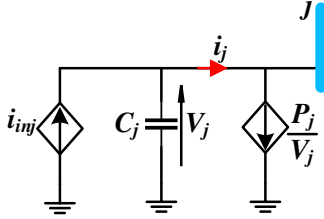
b) Simplified converter model.

Fig. 2: Integration of a DER unit in a meshed DC micro-grid through a power converter.

$\frac{1}{R_{jk}} = 0$. The admittance matrix Y can be rewritten as

$$Y = L - D, \qquad (3)$$

with $D = diag\left\{\frac{P_j}{V_{je}^2}\right\}$ positive-definite and L positive-semidefinite matrices. Note that L represents the Laplacian matrix of the graph $\mathcal{G}$ induced by the DC micro-grid, while D incorporates the self-loops of the nodes.

III. PROPOSED CONTROL ARCHITECTURE

The end goal of this work is to design a primary controller for the DC micro-grid that inherits the conventional and widely used droop controller, whilst guaranteeing an over-voltage protection for each DER unit (node) independently.

The conventional droop control requires each node voltage V_j to satisfy the following expression at the steady-state:

$$V_j = V^* - m_j i_j + x_j^{set}, \qquad (4)$$

where V^* is the rated voltage, m_j is the droop coefficient and x_j^{set} is a desired signal or correction term obtained from the supervisory controller in the hierarchical control architecture. Note that x_j^{set} can be set to 0, which is a common approach in islanded DC micro-grids [23], but generally, it can represent a constant or piecewise constant value (due to the time-scale separation difference between primary and supervisory control).

This paper investigates only the primary control dynamics, and in order to achieve the desired goal, as mentioned above, a novel primary droop control technique is proposed in the sequel.

A. Droop control design with overvoltage protection

Motivated by the development of the sl-PI controller in [21], the proposed droop control strategy defines the control input, i_{inj}, in the following manner:

$$i_{inj} = -g_j V_j + I_{maxj} sin\sigma_j, \qquad (5)$$

with σ_j constructed to follow the nonlinear dynamics

$$\dot{\sigma}_j = \frac{k_j}{I_{maxj}}(V^* - V_j - m_j i_j + x_j^{set})cos\sigma_j, \qquad (6)$$

that incorporates the droop control, with the droop coefficient m_j satisfying the following inequality:

$$m_j < 1. \qquad (7)$$

Substituting the control input from (5) into the open-loop system (1), it yields

$$C_j \dot{V}_j = -g_j V_j + I_{maxj} sin\sigma_j - i_j. \qquad (8)$$

By taking the following continuously differentiable energy-like function for each node j:

$$W_j = \frac{1}{2} C_j V_j^2, \qquad (9)$$

and by calculating its time derivative, it becomes

$$\dot{W}_j = -g_j V_j^2 + V_j I_{maxj} sin\sigma_j - V_j \left(\frac{P_j}{V_j} + \sum_{k\in\mathcal{N}_j} i_{jk}\right)$$

$$= -g_j V_j^2 + V_j I_{maxj} sin\sigma_j - \left(P_j + V_j \sum_{k\in\mathcal{N}_j} i_{jk}\right), (10)$$

where $V_j\sum_{k\in\mathcal{N}_j} i_{jk}$ represents the power fed by the $j-$th converter to the neighbouring converters through every ε_{jk} edge. Considering that $V_j\sum_{k\in\mathcal{N}_j} i_{jk}$ could be both positive or negative, this leads to the scenario where similarly the total power $P_j + V_j\sum_{k\in\mathcal{N}_j} i_{jk}$ could be positive or negative. Hence, the boundedness of the voltage V_j is not straightforward. As a result, the proof can be divided into the two following distinct cases:

a) Case 1: $P_j + V_j\sum_{k\in\mathcal{N}_j} i_{jk} \geq 0$

From equation (10), it is clear that

$$\dot{W}_j \leq -g_j V_j^2 + V_j I_{maxj} sin\sigma_j \leq -g_j|V_j|^2 + I_{maxj}|V_j|. \quad (11)$$

Let $g_j = \bar{g}_j + \epsilon_j > 0$, with $\bar{g}_j > 0$ and ϵ_j representing an arbitrarily small positive constant. In that case, (11) becomes

$$\dot{W}_j \leq -(\bar{g}_j + \epsilon_j)|V_j|^2 + I_{maxj}|V_j|$$

$$\leq -\epsilon_j|V_j|^2, \forall |V_j| \geq \frac{I_{maxj}}{\bar{g}_j}. \qquad (12)$$

According to (12), the solution $V_j(t)$ is uniformly ultimately bounded, and every solution starting with the initial condition $V_j(0)$, satisfying

$$|V_j(0)| \leq \frac{I_{maxj}}{\bar{g}_j}, \qquad (13)$$

will remain in this range for all future time, i.e.

$$|V_j(t)| \leq \frac{I_{maxj}}{\bar{g}_j}, \forall t \geq 0. \qquad (14)$$

To ensure that each voltage V_j is bounded below a maximum voltage V^{max}, the control parameters, $\bar{g}_j$ and I_{maxj} can be selected to satisfy

$$\frac{I_{maxj}}{\bar{g}_j} = V^{max}. \qquad (15)$$

This completes the design of the control parameters $\bar{g}_j$ and I_{maxj}, to guarantee an upper bound for the output voltage V_j, when $P_j + V_j \sum_{k \in \mathcal{N}_j} i_{jk} \geq 0$.

b) Case 2: $P_j + V_j \sum_{k \in \mathcal{N}_j} i_{jk} < 0$

In the islanded microgrid case, considering the existence of constant power loads with $P_j > 0$, at least one converter (e.g. k-th converter) should be feeding the loads and/or other (up to $n - 1$) converter units, based on Kirchhoff's laws. Hence, if the corresponding power of that particular source is $P_k + V_k \sum_{l \in \mathcal{N}_j} i_{kl} > 0$, then since $P_k + V_k \sum_{l \in \mathcal{N}_j} i_{kl} = V_k \left(\frac{P_k}{V_k} + \sum_{l \in \mathcal{N}_j} i_{kl} \right)$, it yields that $V_k > V_l$, and equivalently from *Case 1*, there is $V_k \leq V^{max}$. However, since for the $j-$th source, the output power is negative $P_j < 0$, then there always exists a spanning tree in the induced connected graph $\mathcal{G}$ such that $V_j < V_l < V_k$ which leads to $V_j < V^{max}$.

Therefore, in both cases, an upper bound for the output voltage is guaranteed, i.e. $V_j(t) \leq V^{max}$, at any time instant, i.e., even during transients.

IV. STABILITY ANALYSIS

Prior to proceeding to the stability analysis, let us define the following lemmas:

Lemma 1. Consider A and B two Hermitian matrices, with $\lambda_1 \leq \lambda_2 \leq \ldots \leq \lambda_n$ the eigenvalues of A, and $\beta_1 \leq \beta_2 \leq \ldots \leq \beta_n$ the eigenvalues of B. Then, the following inequality holds

$$\lambda_i + \beta_1 \leq \eta_i \leq \lambda_i + \beta_n,$$

where η_i, with $i \in \mathcal{I}$, represent the eigenvalues of the Hermitian matrix $A + B$.

Proof. presented in Chapter 7, in [24].

Lemma 2. With S a positive-semidefinite real symmetric matrix, and D a positive-definite real symmetric matrix, the following statements hold:

1) SD (or DS) is diagonalizable.
2) SD (or DS) has only real eigenvalues, and same index of inertia as matrix S.

Proof. By polar decomposition SD (or DS) is of the form $SD = UP$, with U unitary and $P = \sqrt{(SD)^T SD}$ is a positive-semidefinite symmetric matrix. Consider Q unitary that satisfies $Q^2 = U$. Note that $M = Q^{-1}(SD)Q = QPQ$ is symmetric, and by spectral decomposition $M = V\Lambda V^{-1}$, with V unitary and Λ diagonal with the eigenvalues of M (and same index of inertia as SD) on the main diagonal. One can infer that $(QV)^{-1} SD (QV) = \Lambda$, with QV unitary. Statement 1) is proved.

Matrix $D^{\frac{1}{2}}(SD)D^{-\frac{1}{2}} = D^{\frac{1}{2}} S D^{\frac{1}{2}}$ is congruent with S, hence, according to Sylvester's law of inertia, SD has the same index of inertia as matrix S. The proof of statement 2) is presented in Chapter 7, in [24].

Consider now the closed-loop micro-grid system written in matrix form:

$$\dot{V} = C^{-1}\left(-gV + I_{max}\mathbf{sin}\sigma - i\right) \tag{16}$$

$$\dot{\sigma} = I_{max}^{-1}k\left[\mathbf{cos}\sigma\right]\left(V^*\mathbf{1}_n - V - mi\right), \tag{17}$$

where $C = diag\{C_j\}$, $V = [V_1 \ldots V_n]$, $g = diag\{g_j\}$, $I_{max} = diag\{I_{maxj}\}$, $i = [i_1 \ldots i_n]$, $\sigma = [\sigma_1 \ldots \sigma_n]$, $k = diag\{k_j\}$, $m = diag\{m_j\}$. Considering an equilibrium point (V_e, σ_e) of the closed-loop system (16)-(17), with $\sigma_{ie} = \left(-\frac{\pi}{2}, \frac{\pi}{2}\right)$, the following theorem can be formulated that guarantees stability of the entire droop-controlled DC microgrid with a CPL.

Theorem 1. The equilibrium point (V_e, σ_e) is asymptotically stable if the controller parameter g_j satisfies

$$g_j > \frac{P_j}{V_{je}^2}, \quad \forall j \in \mathcal{I}. \tag{18}$$

Proof. The corresponding Jacobian matrix of system (16)-(17) has the following form:

$$J = \begin{bmatrix} -C^{-1}g - C^{-1}Y & C^{-1}I_{max}\left[\mathbf{cos}\sigma_e\right] \\ I_{max}^{-1}k\left[\mathbf{cos}\sigma_e\right](D + mY) & \mathbf{0}_{n \times n} \end{bmatrix}.$$

Replacing the admittance matrix Y with its expression from (3), it yields

$$J = \begin{bmatrix} -C^{-1}g - C^{-1}(L - D) & C^{-1}I_{max}\left[\mathbf{cos}\sigma_e\right] \\ I_{max}^{-1}k\left[\mathbf{cos}\sigma_e\right](D + m(L - D)) & \mathbf{0}_{n \times n} \end{bmatrix}.$$

The characteristic polynomial will look as follows:

$$|\lambda I_{2n} - J| = |\lambda^2 I_n + \lambda\mathbf{C} + \mathbf{K}| = 0, \tag{19}$$

with

$$\mathbf{C} = C^{-1}(g + L - D)$$

$$\mathbf{K} = C^{-1}\left[\mathbf{cos}\sigma_e\right]^2 k(mL + (1 - m)D).$$

By left multiplying (19) with $|m^{-1}k^{-1}\left[\mathbf{cos}\sigma_e\right]^{-2}C| > 0$, one obtains

$$|\lambda^2 m^{-1}k^{-1}\left[\mathbf{cos}\sigma_e\right]^{-2}C + \lambda\overline{\mathbf{C}} + \overline{\mathbf{K}}| = 0, \tag{20}$$

with

$$\overline{\mathbf{C}} = m^{-1}k^{-1}\left[\mathbf{cos}\sigma_e\right]^{-2}(g + L - D)$$

$$\overline{\mathbf{K}} = \left(L + m^{-1}(1 - m)D\right).$$

Notice that matrix $\overline{\mathbf{K}}$ is symmetric and matrix $\overline{\mathbf{C}}$ diagonalizable according to Lemma 2, with $P^{-1}\overline{\mathbf{C}}P = \Lambda$, with P unitary and Λ diagonal, having the same index of inertia as matrix $\overline{\mathbf{C}}$. Equation (20) becomes

$$|\lambda^2 m^{-1}k^{-1}\left[\mathbf{cos}\sigma_e\right]^{-2}C + \lambda P^{-1}\Lambda P + \overline{\mathbf{K}}| = 0,$$

or equivalently

$$|\lambda^2 P m^{-1}k^{-1}\left[\mathbf{cos}\sigma_e\right]^{-2}C P^{-1} + \lambda\Lambda + P\overline{\mathbf{K}}P^{-1}| = 0,$$

which is a quadratic eigenvalue problem (QEP) with Λ diagonal having the same index of inertia as matrix $\overline{\mathbf{C}}$, and the similarity transformation $Pm^{-1}k^{-1}\left[\mathbf{cos}\sigma_e\right]^{-2}CP^{-1}$ and $P\overline{\mathbf{K}}P^{-1}$ symmetrical since P is unitary ($P^{-1} = P^T$), and isospectral with $m^{-1}k^{-1}\left[\mathbf{cos}\sigma_e\right]^{-2}C$ and $\overline{\mathbf{K}}$, respectively. According to the QEP theory, if the matrix coefficients are positive-definite, then the eigenvalues are negative, i.e., $\lambda < 0$, thus the Jacobian is Hurwitz. Matrix $m^{-1}k^{-1}\left[\mathbf{cos}\sigma_e\right]^{-2}C$ is already positive definite, hence the two remaining conditions are:
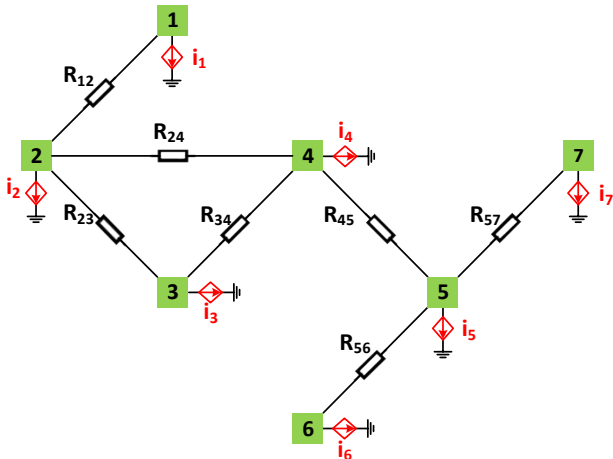
Fig. 3: Meshed DC micro-grid under investigation.

1) $\Lambda \succ 0$, or equivalently $\overline{\mathbf{C}}$ has positive eigenvalues. Since matrix $\overline{\mathbf{C}}$ is represented by a product of two symmetric matrices, one of them being positive-definite, i.e. $m^{-1}k^{-1}\left[\cos\sigma_e\right]^{-2} \succ 0$, according to Sylvester's law of inertia, one can investigate the sign of the remaining symmetric matrix,

$$g + L - D \succ 0.$$

In the worst case scenario, by employing Lemma 1, the above condition becomes in scalar form

$$g_j + 0 - \frac{P_j}{V_{je}^2} > 0,$$

which holds true provided that (18) is satisfied.

2) $\overline{\mathbf{K}} \succ 0$ that, in the worst case scenario according to Lemma 1, in scalar form becomes

$$0 + \frac{1}{m_j}\left(1 - m_j\right)\frac{P_j}{V_{je}^2} > 0,$$

which is true given the appropriate selection of the droop coefficient as specified in (7).

This completes the proof.

V. SIMULATION RESULTS

A DC microgrid portrayed in Figure 3, with the parameters specified in Table I, is considered for simulation testing, consisting of 7 DER units integrated via buck converters, feeding local CPLs, and connected to each other via R_{ij} lines. The expression of the micro-grid's corresponding admittance is introduced at the top of the following page. The main objective of the proposed controller is to regulate each node voltage close to $V^* = 100V$ based on the droop controller concept, while guaranteeing an overvoltage protection.

The system dynamic response is presented in Figure 4. During the first $0.02s$ the converters operate in conventional droop control mode, as the constant correction term $x^{set} = [0\,0\,0\,0\,0\,0\,0]$. Prior to the first load change at $0.01s$, the load power demand is $P = [500\,200\,100\,50\,300\,20\,300]$. The output voltages drop just below the rated value of $100V$ (Figure 4b), as expected by the droop control feature, and
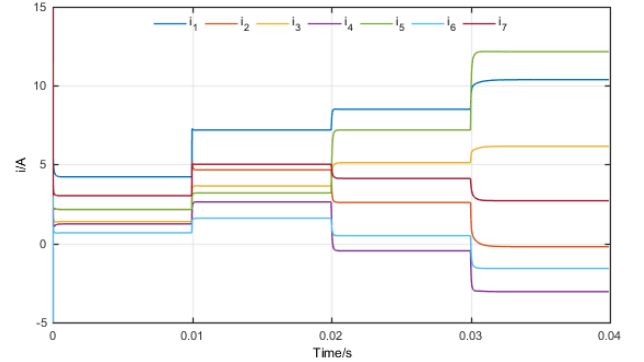
(a) Output currents
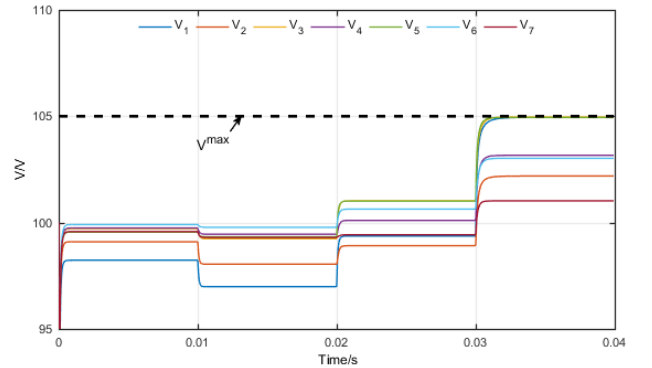
(b) Output voltages

Fig. 4: Simulation results of the DC microgrid equipped with the proposed controller.

the output currents are all positive, thus they all feed their local loads, as it can be observed in Figure 4a.

At $t = 0.01s$, the load power demand increases to $P = [800\,500\,300\,150\,400\,100\,500]$. From Figure 4b, it can be noticed that the output voltages drop even lower than before, while the output currents increase to satisfy the new power demand as reported in Figure 4a.

While maintaining the power demand constant, at $t = 0.02s$, the correction term becomes $x^{set} = [2.94\,0\,2.1\,0\,2.52\,0.7\,0]$, representing possible input signals from a supervisory controller. One can see in Figure 4 that several voltages increase above the rated $100V$, while current i_4 becomes negative. That means that the other six converters are feeding not only the load P_4, but also converter 4.

To test the overvoltage protection, at $t = 0.03s$ the correction term becomes $x^{set} = [10.08\,2.1\,7.56\,2.52\,9.45\,2.8\,1.4]$. The output voltages V_3, V_5, V_6 are successfully limited to

TABLE I: System and control parameters

Parameters	Values
$C\,[\mu F]$	[250 50 200 75 100 350 150]
m	[0.42 0.42 0.21 0.21 0.21 0.14 0.14]
I_{max}	21×10^3
g	200
k	2×10^7
$[R_{12}\,R_{23}\,R_{24}\,R_{34}\,R_{45}\,R_{56}\,R_{57}][\Omega]$	[1 1.5 2 1.25 0.5 0.75 1.75]

$$Y = \begin{bmatrix}
-\frac{P_1}{V_1^2} + \frac{1}{R_{12}} & -\frac{1}{R_{12}} & 0 & 0 & 0 & 0 & 0 \\
-\frac{1}{R_{12}} & -\frac{P_2}{V_2^2} + \left(\frac{1}{R_{12}} + \frac{1}{R_{23}} + \frac{1}{R_{24}}\right) & -\frac{1}{R_{23}} & -\frac{1}{R_{24}} & 0 & 0 & 0 \\
0 & -\frac{1}{R_{23}} & -\frac{P_3}{V_3^2} + \left(\frac{1}{R_{23}} + \frac{1}{R_{34}}\right) & -\frac{1}{R_{34}} & 0 & 0 & 0 \\
0 & -\frac{1}{R_{24}} & -\frac{1}{R_{34}} & -\frac{P_4}{V_4^2} + \left(\frac{1}{R_{24}} + \frac{1}{R_{34}} + \frac{1}{R_{45}}\right) & -\frac{1}{R_{45}} & 0 & 0 \\
0 & 0 & 0 & -\frac{1}{R_{45}} & -\frac{P_5}{V_5^2} + \left(\frac{1}{R_{45}} + \frac{1}{R_{56}} + \frac{1}{R_{57}}\right) & -\frac{1}{R_{56}} & -\frac{1}{R_{57}} \\
0 & 0 & 0 & 0 & -\frac{1}{R_{56}} & -\frac{P_6}{V_6^2} + \frac{1}{R_{56}} & 0 \\
0 & 0 & 0 & 0 & -\frac{1}{R_{57}} & 0 & -\frac{P_7}{V_7^2} + \frac{1}{R_{57}}
\end{bmatrix}$$

$V^{max} = 105V$ (Figure 4b), verifying the developed theory, while the output currents i_2, i_4, i_6 become negative. That is converters 2, 4, 6 and their local loads, P_2, P_4, P_6, are fed by the other four converters.

VI. CONCLUSIONS

In this paper, an enhanced droop controller with overvoltage protection has been presented for meshed DC microgrids consisting of multiple DER units and CPLs. Using nonlinear systems theory, an ultimate bound for the voltage of each source was analytically proven. Closed-loop stability was rigorously guaranteed given some straightforward conditions are met. The theoretical findings and the effectiveness of the proposed approach were verified through simulation testing.

The main aim of this paper was to present for the first time this novel primary droop control structure. Future research will focus on the combination of the proposed controller with supervisory control methods to obtain x^{set} based on centralised or distributed optimal control, in order to finalise the hierarchical control architecture in DC micro-grids.

REFERENCES

[1] J. M. Guerrero, J. C. Vasquez, J. Matas, L. G. de Vicuna, and M. Castilla, "Hierarchical control of droop-controlled ac and dc microgrids 2014; a general approach toward standardization," *IEEE Transactions on Industrial Electronics*, vol. 58, no. 1, pp. 158–172, Jan 2011.

[2] F. Gao, R. Kang, J. Cao, and T. Yang, "Primary and secondary control in dc microgrids: a review," *Journal of Modern Power Systems and Clean Energy*, vol. 7, no. 2, pp. 227–242, Mar 2019. [Online]. Available: https://doi.org/10.1007/s40565-018-0466-5

[3] F. Dorfler and F. Bullo, "Synchronization and transient stability in power networks and nonuniform kuramoto oscillators," *SIAM Journal on Control and Optimization*, vol. 50, no. 3, pp. 1616–1642, 2012.

[4] V. Mariani, F. Vasca, J. C. Vásquez, and J. M. Guerrero, "Model order reductions for stability analysis of islanded microgrids with droop control," *IEEE Transactions on Industrial Electronics*, vol. 62, no. 7, pp. 4344–4354, 2015.

[5] J. W. Simpson-Porco, F. Dörfler, and F. Bullo, "Voltage stabilization in microgrids via quadratic droop control," *IEEE Transactions on Automatic Control*, vol. 62, no. 3, pp. 1239–1253, March 2017.

[6] A. P. N. Tahim, D. J. Pagano, E. Lenz, and V. Stramosk, "Modeling and stability analysis of islanded DC microgrids under droop control," *IEEE Transactions on Power Electronics*, vol. 30, no. 8, pp. 4597–4607, Aug 2015.

[7] A. Emadi, A. Khaligh, C. H. Rivetta, and G. A. Williamson, "Constant power loads and negative impedance instability in automotive systems: definition, modeling, stability, and control of power electronic converters and motor drives," *IEEE Transactions on Vehicular Technology*, vol. 55, no. 4, pp. 1112–1125, July 2006.

[8] D. Marx, P. Magne, B. Nahid-Mobarakeh, S. Pierfederici, and B. Davat, "Large signal stability analysis tools in DC power systems with constant power loads and variable power loads—a review," *IEEE Transactions on Power Electronics*, vol. 27, no. 4, pp. 1773–1787, April 2012.

[9] M. Cespedes, L. Xing, and J. Sun, "Constant-power load system stabilization by passive damping," *IEEE Transactions on Power Electronics*, vol. 26, no. 7, pp. 1832–1836, July 2011.

[10] A. Kwasinski and C. N. Onwuchekwa, "Dynamic behavior and stabilization of DC microgrids with instantaneous constant-power loads," *IEEE Transactions on Power Electronics*, vol. 26, no. 3, pp. 822–834, March 2011.

[11] W. Lee and S. Sul, "DC-link voltage stabilization for reduced dc-link capacitor inverter," *IEEE Transactions on Industry Applications*, vol. 50, no. 1, pp. 404–414, Jan 2014.

[12] P. Magne, B. Nahid-Mobarakeh, and S. Pierfederici, "DC-link voltage large signal stabilization and transient control using a virtual capacitor," in *2010 IEEE Industry Applications Society Annual Meeting*, Oct 2010, pp. 1–8.

[13] E. Coyne, D. Clarke, S. Heffernan, and B. Moane, "Designing ESD protection devices for ultrafast overvoltage events," *IEEE Transactions on Electron Devices*, vol. 66, no. 11, pp. 4850–4857, Nov 2019.

[14] F. Zhang, X. Duan, M. Liao, J. Zou, and Z. Liu, "Statistical analysis of switching overvoltages in UHV transmission lines with a controlled switching," *IET Generation, Transmission Distribution*, vol. 13, no. 21, pp. 4998–5004, 2019.

[15] P. D. F. Ferreira, P. M. S. Carvalho, L. A. F. M. Ferreira, and M. D. Ilic, "Distributed energy resources integration challenges in low-voltage networks: Voltage control limitations and risk of cascading," *IEEE Transactions on Sustainable Energy*, vol. 4, no. 1, pp. 82–88, Jan 2013.

[16] P. N. Vovos, A. E. Kiprakis, A. R. Wallace, and G. P. Harrison, "Centralized and distributed voltage control: Impact on distributed generation penetration," *IEEE Transactions on Power Systems*, vol. 22, no. 1, pp. 476–483, Feb 2007.

[17] Y. Ueda, K. Kurokawa, T. Tanabe, K. Kitamura, and H. Sugihara, "Analysis results of output power loss due to the grid voltage rise in grid-connected photovoltaic power generation systems," *IEEE Transactions on Industrial Electronics*, vol. 55, no. 7, pp. 2744–2751, July 2008.

[18] R. Tonkoski, L. A. C. Lopes, and T. H. M. El-Fouly, "Coordinated active power curtailment of grid connected PV inverters for overvoltage prevention," *IEEE Transactions on Sustainable Energy*, vol. 2, no. 2, pp. 139–147, April 2011.

[19] H. Chen, P. D. S. Assala, Y. Cai, and P. Yang, "Intelligent transient overvoltages location in distribution systems using wavelet packet decomposition and general regression neural networks," *IEEE Transactions on Industrial Informatics*, vol. 12, no. 5, pp. 1726–1735, Oct 2016.

[20] S. Beheshtaeina, M. Savaghebia, R. Cuznerb, and J. M. Guerreroa, "A hierarchical multiagent-based protection structure for meshed microgrids," in *IECON 2018 - 44th Annual Conference of the IEEE Industrial Electronics Society*, 2018, pp. 45–52.

[21] G. C. Konstantopoulos and P. R. Baldivieso-Monasterios, "State-limiting PID controller for a class of nonlinear systems with constant uncertainties," *International Journal of Robust and Nonlinear Control*, vol. n/a, no. n/a, 2019. [Online]. Available: https://onlinelibrary.wiley.com/doi/abs/10.1002/rnc.4853

[22] F. Dorfler and F. Bullo, "Kron reduction of graphs with applications to electrical networks," *IEEE Transactions on Circuits and Systems I: Regular Papers*, vol. 60, no. 1, pp. 150–163, 2013.

[23] A. C. Braitor, G. C. Konstantopoulos, and V. Kadirkamanathan, "Current-limiting droop control design and stability analysis for paralleled boost converters in DC microgrids," *IEEE Transactions on Control Systems Technology*, pp. 1–10, 2020.

[24] C. D. Meyer, *Matrix Analysis and Applied Linear Algebra*. Philadelphia: Society for Industrial and Applied Mathematics, 2000.